Power Flow Analysis of Islanded AC Microgrids

Elefherios O. Kontis, Georgios C. Kryonidis, Angelos I. Nousdilis,
Kyriaki-Nefeli D. Malamaki, and Grigoris K. Papagiannis
School of Electrical and Computer Engineering,
Aristotle University of Thessaloniki,
Thessaloniki, Greece

***Abstract*—This paper presents a methodology for the steady-state analysis, i.e., power flow analysis, of islanded AC microgrids (MGs), operated under the droop control scheme. In the proposed framework, the power flow is computed using conventional power flow methods. For this purpose, a slack bus is considered to be connected to a random node of the examined MG. Subsequently, an iterative procedure is applied to determine the operational conditions, i.e., voltage level, frequency, active and reactive power absorption/injection, of this slack bus as well as of the rest MG nodes. The objective of the proposed iterative procedure is to force active and reactive power, flowing through the slack bus, to zero, emulating this way the islanded operation of the MG. To evaluate the performance of the proposed methodology, time-domain simulations are conducted on a low-voltage MG, using detailed models for all system components. The corresponding results are compared with those derived using the proposed methodology. In all cases, trivial differences are observed, validating the accuracy and the robustness of the proposed approach.**

***Index Terms*—Droop control method, dynamic analysis, islanded microgrids, power flow analysis.**

I. Introduction

To facilitate the dynamic and steady-state analysis of MGs, several mathematical models and techniques have been proposed in the literature [1]. Concerning steady state analysis, power flow tools are essential for the secure and reliable operation of MGs [2], [3]. These tools can be used for planning purposes, network optimization, reconfiguration studies, security analysis as well as for the initialization of system dynamic analysis [3].

The power flow problem can be easily tackled in grid-connected MGs by applying conventional power flow (CPF) methods, such as the Newton Raphson and the Gauss-Seidel [4]. These methods are based on the concept of the slack bus, which is used to simulate the utility grid [4]. In particular, the slack bus imitates the behavior of a large synchronous machine, providing/absorbing the deficit/surplus of active and/or reactive power. In this concept, the grid frequency is predetermined, while voltage magnitude of the slack bus is assumed constant and *a priori* known. Distributed generation (DG) units are represented as PV or PQ buses [5], [6], i.e., as buses with pre-specified active power and voltage magnitude or buses with pre-specified active and reactive power.

However, CPF methods cannot be used for the analysis of droop-controlled islanded MGs [7], [8]. The modeling of these systems differs from grid-connected MGs in the following aspects: a) In these systems, the concept of a slack bus operating at fixed frequency and voltage is not valid [2], since node voltages and network frequency are determined by the operating conditions of the MG loads and DG units and they are controlled by the corresponding droop characteristics [7], [8]. b) Network reactances cannot be considered constant, since they are considerably affected by the frequency changes.

A potential solution involves the detailed modeling of the examined MG in standard time-domain (TD) simulation software, such as PSCAD, Simulink, PSIM, among others, and the simulation of the MG behavior until the transient phase is damped out [9]. This approach provides very accurate and reliable results. However, the calculation of the steady-state solution using TD simulations generally requires high execution times [9]. Hence, the applicability of this approach for the analysis of large-scale MGs is highly questionable.

To avoid time-consuming TD simulations and to facilitate the power flow analysis of AC islanded MGs, several approaches have been proposed in the literature [2], [8]–[16]. More specifically, a particle swarm optimization method is proposed in [2]. However, as discussed in [10], the use of evolutionary methods for power flow calculation may lead to considerably high execution times as well as to inconsistent results due to initialization failures. In [8] and [11], modified Newton Raphson methods are implemented. These methods are accurate but they are characterized by increased computational burden, since they require the inverse of the Jacobian Matrix. In [12], a Newton trust-region method is proposed for the power flow analysis of balanced and unbalanced islanded MGs. The method is based on nonlinear equations, used to simulate the operating modes of DG units. The method is accurate but computationally intensive for extended MGs. In [13]–[15], modified backward-forward sweep load flow methods for islanded MGs are proposed. These methods are fast and accurate but they can only be applied for the analysis of radial or weakly-meshed distribution grids [17]. In our

This research is carried out / funded in the context of the project "Advanced co-simulation techniques for smart grids" (MIS Code: 5004907) under the call for proposals "Supporting researchers with emphasis on new researchers" (EDULLL 34). The project is co-financed by Greece and the European Union (European Social Fund - ESF) by the Operational Programme Human Resources Development, Education and Lifelong Learning 2014-2020.

All data underpinning this publication are openly available from the Power Systems Laboratory of Aristotle University of Thessaloniki at http://power.ee.auth.gr.

Citation Information: DOI: 10.1109/PTC.2019.8810612

previous work [16], a novel methodology, based on a two-nested-loop iterative procedure, was developed to extend the applicability of CPF methods for droop-based islanded MGs. The frequency of the MG and active power injections of the DG units are computed in the first loop. Afterwards, the second loop is used to calculate node voltages and reactive power injections of the DG units. However, modeling of voltage dependent droop curves using iterative procedures, may result in numerical oscillations of the injected power and network voltages. As discussed in [18] and [19], in extended networks with high penetration of DG units, these spurious oscillations may lead to convergence issues. Therefore, in these cases, the method of [16] may fail to provide consistent results.

To overcome this issue, in this paper, the method of [16] is further extended to enhance the power flow analysis of large-scale islanded MGs. Towards this objective, a third loop is added in the formulation of [16]. The aim of this loop is to simulate with higher accuracy the $Q-V$ droop control. The performance of the proposed methodology is evaluated on a low-voltage (LV) MG by means of TD simulations conducted using the PSIM software. The examined LV MG constitutes a modified version of the European LV residential distribution grid proposed by Cigre Task Force C6.04 [20]. Grid and converter models are modelled with high details, aiming to develop a benchmark LV MG suitable for the testing and analysis of power flow methodologies oriented to the analysis of islanded MGs.

II. Droop-based Islanded MGs

The power sharing of active and reactive power among the DG units of islanded MGs can be achieved using the $P-f$ and $Q-V$ droop curves, respectively [21]. These droop curves, can be mathematically expressed using the following set of equations:

$$f_{grid} = f_{\max} - m_i P_i \quad \forall i \in N_{dg} \tag{1}$$

$$V_i = V_{\max} - n_i(Q_i + Q_{\max,i}) \quad \forall i \in N_{dg} \tag{2}$$

where

$$m_i = \frac{f_{max} - f_{min}}{P_{max,i}} \quad \forall i \in N_{dg} \tag{3}$$

$$n_i = \frac{V_{max} - V_{min}}{2Q_{max,i}} \quad \forall i \in N_{dg}. \tag{4}$$

Here, N_{dg} denotes the number of the installed DG units. V_{max}, V_{min}, f_{max} and f_{min} are the maximum and minimum operational limits of voltage and frequency, respectively. In this paper, these limits are defined according to Standard EN50160 [22]. Additionally, $Q_{max,i}$ is the maximum available reactive power of the i-th DG unit, while P_i and Q_i are the injected active and reactive power of the i-th unit, respectively. m_i and n_i are the corresponding droop coefficients [21].

III. Proposed Method

As discussed in the introduction, CPF methods cannot be used for the power flow analysis of islanded MGs, since they require the existence of a slack bus, operating at constant and pre-determined voltage and frequency. Therefore, to apply these methods for the power flow analysis of islanded MGs, the operational conditions of the slack bus must be available prior to the power flow solution [16]. To address this issue, in this paper, the three-nested-loop iterative procedure of Fig. 1 is proposed. The objective of this iterative procedure is to properly adjust the network frequency (f_{grid}) and the voltage magnitude of the slack bus (V_{sb}) in order to force active and reactive power flowing through the slack bus to zero, emulating this way the islanded operation mode. The proposed iterative method consists of the following steps:

Step-1: The initial conditions are applied. In particular, V_{sb} and f_{grid} receive the maximum permissible values, i.e. V_{max} and f_{max}, respectively. Additionally, variables V_{ub} and V_{lb} are set equal to V_{max} and V_{min}, respectively. A further insight on these variables will be given in Step-13. For the initialization, the active power injections of all DG units are considered equal to zero, while reactive power injections are considered equal to $-Q_{max,i}$. In each power flow calculation, active and reactive power injections are stored in two discrete vectors denoted for the rest of the paper as $\boldsymbol{P}_{dg}$ and $\boldsymbol{Q}_{dg}$, respectively. Additionally, at this step, the user defines the value of the integral term k, used to calculate reactive power injections of DG units. A further insight on this integral term is provided in Step-9. Finally, at this step, the user defines the maximum number of iterations, i.e., $MaxIter$, and the tolerances for the convergence of the three loops, i.e. $tolp$, $tolv$, $tolq$.

Step-2: Line and load impedances are computed at f_{grid}.

Step-3: Subsequently, a power flow analysis is performed and the value of counter c is set to 1. This counter is used to monitor the number of iterations performed during the second loop of the proposed algorithm. Further information concerning this counter can be found in Steps 6 to 11.

Step-4: The active power flowing through the slack bus (P_{sb}) as well as the network voltages ($\boldsymbol{V}^c$) are computed.

Step-5: A convergence check is performed to evaluate if the absolute value of P_{sb}, i.e., $|P_{sb}|$, is greater than the predefined tolerance $tolp$. If so, P_{sb} must be reallocated to all installed DG units in order to zero the active power flowing through the slack bus. To achieve this objective, all DG units must adjust their injected active power by a ΔP_i amount. This amount can be mathematically expressed using (5) and (6). Please note that (6) is imposed due to the use of the droop control mechanism [10]. Then, vector $\boldsymbol{P}_{dg}$ is updated by adding the corresponding ΔP_i amounts. Subsequently, the new f_{grid} is calculated using (1) and the procedure moves back to Step 2. Then, a new power flow is performed using the updated values of $\boldsymbol{P}_{dg}$ and f_{grid}. When $|P_{sb}|$ becomes lower than $tolp$, the algorithm moves to Step-6.

Step-6: The value of counter c is increased by one.

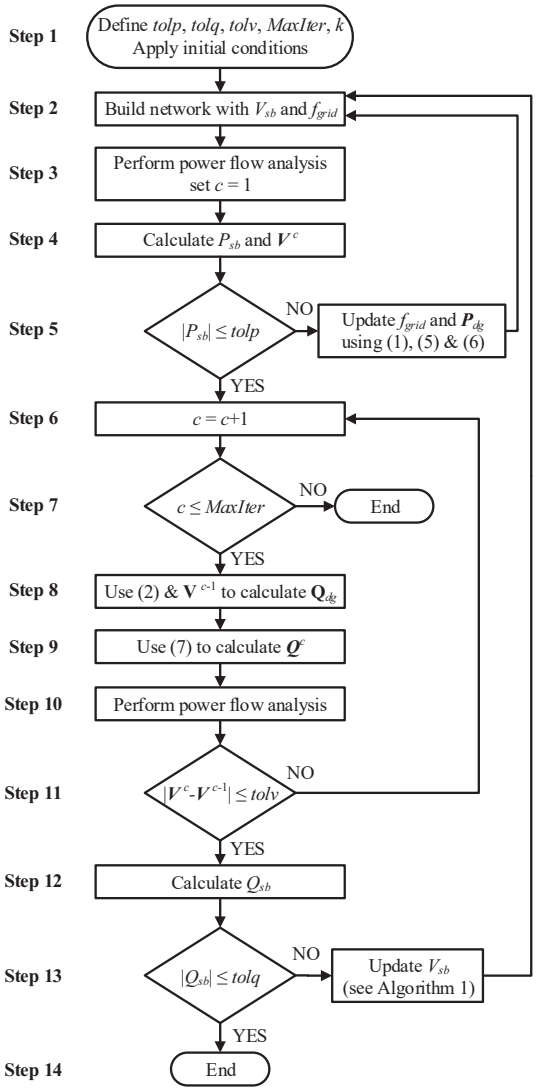

Fig. 1. Flowchart of the proposed method.

$$\sum_{i=1}^{N_{dg}} \Delta P_i = P_{sb} \tag{5}$$

$$m_1 \Delta P_1 = ... = m_{N_{dg}} \Delta P_{N_{dg}} \tag{6}$$

Step-7: If c is greater than the predefined maximum number of iterations, i.e., $MaxIter$, the algorithm terminates, since convergence cannot be achieved. To address this issue, the user should repeat the power flow analysis using a higher value for the integral term k. A detailed analysis for the impact of the integral term on the convergence of the proposed method is presented in Step-9.

Step-8: Reactive power injections of all DG units, i.e., $\boldsymbol{Q}_{dg}$, are computed according to (2), using $\boldsymbol{V}^{c-1}$.

Step-9: Modeling of voltage dependent droop curves using iterative procedures, may result in numerical oscillations of the injected powers. These power oscillations result in voltage oscillations [18], [19]. To avoid these spurious oscillations, in this paper, the approach of [18] is adopted. More specifically,

Algorithm 1 Binary search for V_{sb}

```
if Q_sb > 0 then
    set V_sb^n to V_sb^p − (V_sb^p − V_lb^p)/2, V_lb^n to V_lb^p, V_ub^n to V_sb^p
else
    set V_sb^n to V_sb^p + (V_ub^p − V_sb^p)/2, V_lb^n to V_sb^p, V_ub^n to V_ub^p
end if
```

the power flow is not performed using $\boldsymbol{Q}_{dg}$ injections. On the contrary, for the c-th iteration, the injected reactive powers $\boldsymbol{Q}^c$ are computed taking into account the values of the previous iteration $\boldsymbol{Q}^{c-1}$, the values of $\boldsymbol{Q}_{dg}$ as well the value of the integral term k. $\boldsymbol{Q}^c$ is computed as follows:

$$\boldsymbol{Q}^c = \boldsymbol{Q}^{c-1} + \frac{\boldsymbol{Q}_{dg} - \boldsymbol{Q}^{c-1}}{k} \tag{7}$$

The value of k can vary from small to large values. Small values result in small execution times, but cannot guarantee the convergence. On the other hand, large values exhibit slow convergence rate, but result in more robust and accurate results [18], [19].

Step-10: Voltages of all MG nodes, i.e., $\boldsymbol{V}^c$, are computed through a power flow analysis using $\boldsymbol{P}_{dg}$, $\boldsymbol{Q}^c$, and f_{grid}.

Step-11: A comparison of all node voltages between the last two iterations is performed. If $tolv$ criterion is satisfied, the algorithm proceeds to Step-12, otherwise the algorithm moves back to Step-6 and new reactive power injections are computed.

Step-12: Using the results of the last power flow, the reactive power flowing through the slack bus, i.e., Q_{sb}, is calculated.

Step-13: If the absolute value of Q_{sb}, i.e. $|Q_{sb}|$, is less than $tolq$, the algorithm moves to Step-14 and terminates. Otherwise, a new V_{sb} must be defined to zero the reactive power flowing through the slack bus. More specifically, a negative Q_{sb} value indicates a surplus of reactive power in the MG, absorbed from the slack bus. Therefore, according to (2), V_{sb} must be increased to force DG units to reduce their reactive power injection. On the contrary, if Q_{sb} is positive, V_{sb} must be reduced. The new value of V_{sb} is determined through a binary search method [16]. The binary search algorithm is presented in Algorithm 1. In Algorithm 1, V_{ub} and V_{lb} are the upper and lower limits of the searching interval, while p and n are the corresponding previous and new values. Once the new V_{sb} is defined, the procedure moves back to Step-2.

Step-14: The procedure terminates providing the power flow solution of the examined MG.

IV. System Under Study

The system under study is presented in Fig. 2 and consists of a 0.4 kV islanded MG. This system is based on the topology of the European LV residential distribution grid [20]. The notation and the numbering of nodes in Fig. 2 is according to [20]. To derive the LV MG, the following modifications have been applied on the benchmark model of [20]. First, six (6) DG units are connected to nodes R2, R5, R7, R10, R12, and R15. The droop coefficients of all DG units are presented

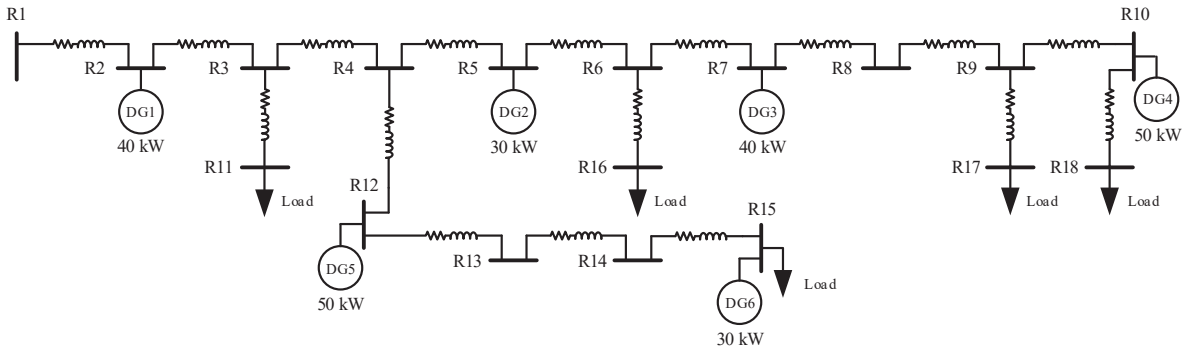

Fig. 2. Examined LV MG.

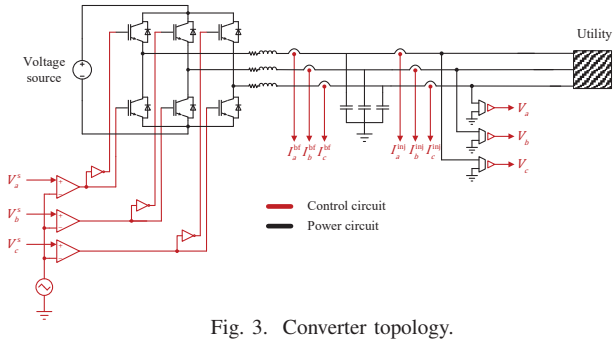

Fig. 3. Converter topology.

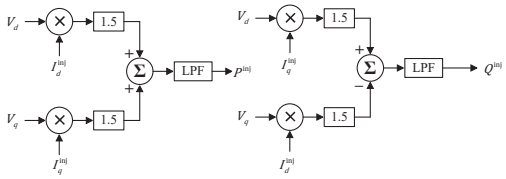

Fig. 4. Active and reactive power calculation.

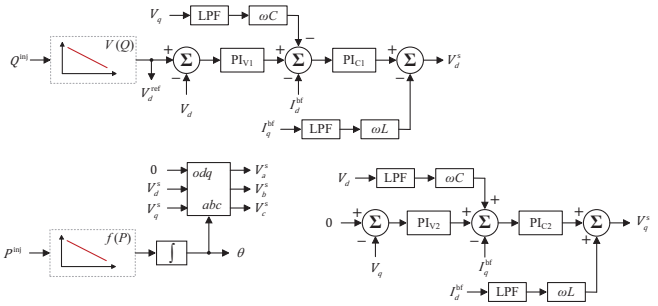

Fig. 5. Control process.

TABLE II
SETTINGS OF PI CONTROLLERS

Parameters	$\mathbf{PI}_{V1}$	$\mathbf{PI}_{V2}$	$\mathbf{PI}_{C1}$	$\mathbf{PI}_{C2}$
K_p	0.45	0.45	0.1	0.1
K_i	4.5	4.5	20	20

in Table I. Additionally, the load connected in node R1 of the benchmark system is intentionally omitted from the LV MG of Fig. 2. As discussed in [20], this load represents additional feeders served by dedicated transformers, i.e. this load does not constitute a part of the examined feeder. Thereby it is omitted from the analysis. All other network loads as well as network lines are modeled as discussed in [20].

Details concerning the modeling of the converters, used for the interconnection of the DG units, are provided in Figs. 3 to 5. In particular, the topology of the employed converter is presented in Fig. 3, where the power circuit is depicted with black lines and the control circuit with red lines. V_a^s, V_b^s, and V_c^s denote the voltage control signals in the *abc* framework, while V_a, V_b, and V_c are the corresponding grid voltages. I_a^{bf}, I_b^{bf}, and I_c^{bf} are the currents before the LC filter, while I_a^{inj}, I_b^{inj}, and I_c^{inj} denote the current injections at the grid in the *abc* framework. The inductance (L) and the capacitor (C) of all LC filters are equal to 2 mH and 15.5 μF, respectively. The transition frequency of the switches for all DG converters is set to 9950 Hz. The injected active and reactive powers are computed as presented in Fig. 4, where V_d, V_q, I_d^{inj} and I_q^{inj} denote grid voltages and current injections in the 0*dq* framework, respectively. Abbreviation LPF denotes the existence of a low pass filter. The cutoff frequency for all LPFs is equal to 10 Hz. Control signals are computed based on the approach presented in Fig. 5. Here, I_d^{bf} and I_q^{bf} denote the total current injection in the 0*dq* system, while V_d^s and V_q^s the corresponding voltage control signals. ω is the angular frequency and θ the corresponding angle between 0*dq* and *abc* reference frames. PI_{V1}, PI_{C1}, PI_{V2}, and PI_{C2} denote the required PI controllers. The corresponding settings are presented in Table II.

TABLE I
DROOP COEFFICIENTS m (HZ/KW) & n (V/KVAR)

Coefficient	DG1	DG2	DG3	DG4	DG5	DG6
m_i	0.050	0.066	0.050	0.040	0.040	0.066
n_i	1.613	2.151	1.613	1.291	1.291	2.151

V. Numerical Validation

A. Time-domain Simulations

Initially the LV MG of Fig. 2 is implemented in full detail in the PSIM software and the power flow problem is solved by performing TD simulations. The developed models can be found in [23]. Dynamic responses of active and reactive power injections of all DG units as well as the dynamic response of MG frequency are presented in Figs. 6a to 6c, respectively. Based on these results, it can be perceived that the steady-state of the MG is established approximately at around t=3 s. However, to ensure that all dynamic phenomena have been properly damped, the TD simulation continues up to t=25 s. To simulate the first three seconds and to reach the steady-state condition, PSIM requires approximately 2958 s. All simulations were conducted using an Intel Core i7-930, 2.8 GHz, RAM 24 GB, personal computer.

The MG frequency in the new steady-state is equal to 49.36869 Hz. Active and reactive power injections of all DG units are reported in Table III, while the voltage profile along the MG is presented in Fig. 7.

B. Simulation Results

In this subsection the proposed method is implemented using the MATLAB and the OpenDSS software. The former is used to implement the flowchart of Fig. 1, while the latter is utilized as a phase-domain power flow solver [18]. $tolp$, $tolq$ and $tolv$ are set to 0.1 W, 0.1 VAr, and 0.00001 V, respectively. $MaxIter$ and k are assumed equal to 100 and 2, respectively.

Initially, the slack bus is randomly placed at node R1. The total execution time of the proposed method is 11.3 s. The MG frequency, as calculated by the proposed method, is equal to 49.36874 Hz. Compared to detailed TD simulations an absolute percentage error equal to 0.00012 % is observed. Active and reactive power injections of all DG units are listed in Table III. As shown, a near-zero mismatch, compared to TD simulations, is observed. Additionally, the voltage profile

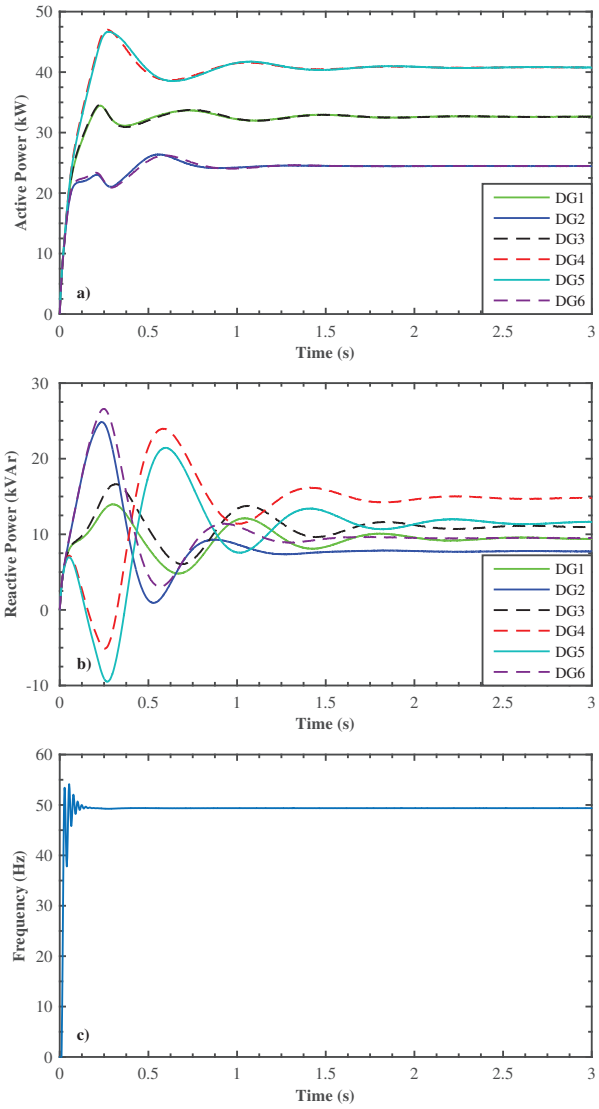

Fig. 6. Dynamic responses of a) active power injections, b) reactive power injections, and c) MG frequency.

TABLE III
Active (kW) and Reactive (kVAr) Power of DG Units

	P_1	P_2	P_3
PSIM	32.625001	24.468759	32.625001
Proposed	32.625803	24.469317	32.625755
	P_4	P_5	P_6
PSIM	40.781265	40.781265	24.468759
Proposed	40.782290	40.782270	24.469311
	Q_1	Q_2	Q_3
PSIM	9.451056	7.750209	10.993335
Proposed	9.450450	7.750154	10.993439
	Q_4	Q_5	Q_6
PSIM	14.785813	11.55335	9.511234
Proposed	14.786397	11.55284	9.511380

along the MG is depicted in Fig. 7. Once again, only trivial differences compared to TD simulations are recorded, validating the accuracy of the proposed method. Indeed, the maximum absolute percentage error between the TD simulation and the proposed method is only 0.026 % and observed for node R1.

The proposed method yields almost identical results regardless the location of the slack bus. To further support this argument, the power flow solution is derived assuming different locations for the slack bus. More specifically, eighteen distinct test cases are considered. In each test case, the slack bus is assumed to be connected at a different MG node. The mean execution time of the eighteen power flows is 11.19 s, validating the low computational burden of the proposed method. For each test case, the absolute percentage errors, concerning the voltage magnitude of all MG nodes, between the proposed method and the TD simulation, are computed. The corresponding results are analyzed in the boxplots of

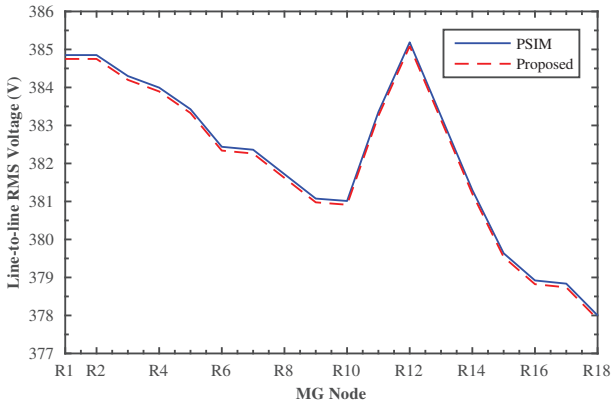

Fig. 7. Voltage profile along the MG.

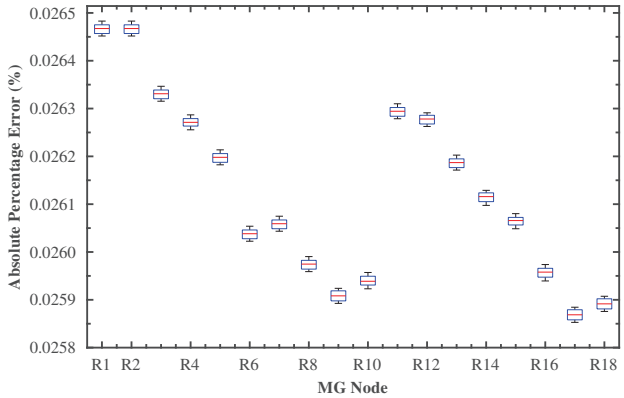

Fig. 8. Absolute percentage errors of voltage magnitudes of all MG nodes, assuming different locations for the slack bus.

Fig. 8. In all cases, regardless the location of the slack bus, trivial differences are observed.

VI. Conclusions

In this paper, a new method is proposed to accurately solve the power flow problem of islanded AC MGs. Towards this objective, a three-nested-loop iterative procedure is developed to extend the applicability of CPF methods for the analysis of islanded MGs. The performance of the proposed method is validated on an eighteen-bus LV MG using TD simulations. In all test cases, the method results in very accurate and robust estimates, presenting also low computational burden. Therefore, it can be concluded that the proposed method constitutes a reliable tool which can be used for the power flow analysis of islanded MGs.

Future work will be conducted to extend the applicability of the developed method for the analysis of unbalanced MGs as well as for the analysis of islanded MGs operated with hierarchical control. Finally, further steps aim to include the virtual impedance concept in the proposed formulation.

References

[1] D. E. Olivares, A. Mehrizi-Sani, A. H. Etemadi, C. A. Caizares, R. Iravani, M. Kazerani, A. H. Hajimiragha, O. Gomis-Bellmunt, M. Saeedifard, R. Palma-Behnke, G. A. Jimnez-Estvez, and N. D. Hatziargyriou, "Trends in microgrid control," *IEEE Trans. Smart Grid*, vol. 5, no. 4, pp. 1905–1919, July 2014.

[2] A. Elrayyah, Y. Sozer, and M. E. Elbuluk, "A novel load-flow analysis for stable and optimized microgrid operation," *IEEE Trans. Power Del.*, vol. 29, no. 4, pp. 1709–1717, Aug. 2014.

[3] C. Li, S. K. Chaudhary, M. Savaghebi, J. C. Vasquez, and J. M. Guerrero, "Power flow analysis for low-voltage ac and dc microgrids considering droop control and virtual impedance," *IEEE Trans. Smart Grid*, vol. 8, no. 6, pp. 2754–2764, Nov. 2017.

[4] H. Saadat, *Power System Analysis*. New York: McGraw-Hill, 1999.

[5] H. Nikkhajoei and R. Iravani, "Steady-state model and power flow analysis of electronically-coupled distributed resource units," *IEEE Trans. Power Del.*, vol. 22, no. 1, pp. 721–728, Jan. 2007.

[6] M. Z. Kamh and R. Iravani, "Unbalanced model and power-flow analysis of microgrids and active distribution systems," *IEEE Trans. Power Del.*, vol. 25, no. 4, pp. 2851–2858, Oct. 2010.

[7] ——, "A sequence frame-based distributed slack bus model for energy management of active distribution networks," *IEEE Trans. Smart Grid*, vol. 3, no. 2, pp. 828–836, June 2012.

[8] M. A. Allam, A. A. Hamad, and M. Kazerani, "A generic modeling and power-flow analysis approach for isochronous and droop-controlled microgrids," *IEEE Trans. Power Syst.*, vol. 33, no. 5, pp. 5657–5670, Sept. 2018.

[9] G. Agundis-Tinajero, J. Segundo-Ramrez, N. Visairo-Cruz, M. Savaghebi, J. M. Guerrero, and E. Barocio, "Power flow modeling of islanded ac microgrids with hierarchical control," *Int. J. Electr. Power Energy Syst.*, vol. 105, pp. 28–36, 2019.

[10] M. H. Moradi, V. B. Foroutan, and M. Abedini, "Power flow analysis in islanded micro-grids via modeling different operational modes of dgs: A review and a new approach," *Renewable Sustain. Energy Rev.*, vol. 69, pp. 248–262, Nov. 2017.

[11] F. Mumtaz, M. H. Syed, M. A. Hosani, and H. H. Zeineldin, "A novel approach to solve power flow for islanded microgrids using modified newton raphson with droop control of dg," *IEEE Trans. Sustai. Energy*, vol. 7, no. 2, pp. 493–503, Apr. 2016.

[12] M. M. A. Abdelaziz, H. E. Farag, E. F. El-Saadany, and Y. A. I. Mohamed, "A novel and generalized three-phase power flow algorithm for islanded microgrids using a newton trust region method," *IEEE Trans. Power Syst.*, vol. 28, no. 1, pp. 190–201, Feb. 2013.

[13] F. Hameed, M. A. Hosani, and H. H. Zeineldin, "A modified backward/forward sweep load flow method for islanded radial microgrids," *IEEE Trans. Smart Grid*, in press 2018.

[14] L. Ren and P. Zhang, "Generalized microgrid power flow," *IEEE Trans. Smart Grid*, vol. 9, no. 4, pp. 3911–3913, July 2018.

[15] M. Nassar and M. M. A. Salama, "A novel branch-based power flow algorithm for islanded ac microgrids," *Elect. Power Syst. Res.*, vol. 146, pp. 51–62, May 2017.

[16] G. C. Kryonidis, E. O. Kontis, A. I. Chrysochos, K. O. Oureilidis, C. S. Demoulias, and G. K. Papagiannis, "Power flow of islanded ac microgrids: Revisited," *IEEE Trans. Smart Grid*, vol. 9, no. 4, pp. 3903–3905, July 2018.

[17] G. X. Luo and A. Semlyen, "Efficient load flow for large weakly meshed networks," *IEEE Trans. Power Syst.*, vol. 5, no. 4, pp. 1309–1316, Nov. 1990.

[18] G. C. Kryonidis, E. O. Kontis, A. I. Chrysochos, C. S. Demoulias, D. Bozalakov, B. Meersman, T. L. Vandoorn, and L. Vandevelde, "A simulation tool for extended distribution grids with controlled distributed generation," in *2015 IEEE Eindhoven PowerTech*, June 2015.

[19] D. Fetzer, G. Lammert, S. Gehler, J. Hegemann, R. Schmoll, and M. Braun, "Integration of voltage dependent power injections of distributed generators into the power flow by using a damped newton method," *Int. J. Electr. Power Energy Syst.*, vol. 99, pp. 695–705, 2018.

[20] *Benchmark Systems for Network Integration of Renewable and Distributed Energy Resources*. Cigre Task Force C6.04, Technical Report, 2014.

[21] J. M. Guerrero, M. Chandorkar, T. Lee, and P. C. Loh, "Advanced control architectures for intelligent microgrids - Part I: Decentralized and hierarchical control," *IEEE Trans. Ind. Elect.*, vol. 60, no. 4, pp. 1254–1262, Apr. 2013.

[22] *Voltage Characteristics of Electricity Supplied by Public Distribution Networks*, Standard EN 50160, 2010.

[23] http://power.ee.auth.gr/.